Sorption–Deformation–Percolation Model for Diffusion in Nanoporous Media

Chi Zhang, Ali Shomali, Benoit Coasne, Dominique Derome, Jan Carmeliet

Adsorption/percolation model for water diffusion in deformable nanoporous polymers

Chi Zhang[†*], *Ali Shomali, Benoit Coasne*[‡], *Dominique Derome*[§], *Jan Carmeliet*[†]

[†] Chair of Building Physics, Department of Mechanical and Process Engineering, ETH Zurich, Raemistrasse 101, 8092 Zurich, Switzerland.

[‡] Université Grenoble Alpes, CNRS, LIPhy, 38000 Grenoble, France

[§] Department of Civil and Building Engineering, Université de Sherbrooke, Sherbrooke J1K 2R1, Québec, Canada

* Corresponding Email: outlook.zhangchi@gmail.com

Abstract

Molecules diffusing in porous media exhibit complex dynamics when their size approaches the pore length scale and strong guest-host forces are at play – as is the case for water diffusion in a dense, adsorbing and deformable polymer. The intricate nature of diffusion impedes the complete understanding of the mechanisms, despite the fundamental relevance to numerous important applications. Here, molecular dynamics simulations are used to formulate a theoretical framework that sheds light on the intermittent dynamics of confined water molecules and its link with the material structure as well as its physical behavior (sorption and deformation). By analyzing water trajectories, we determine the moving and waiting times as well as the switching frequency to predict the microscopic self-diffusion coefficient. The apparent tortuosity, defined as the ratio of the bulk to the confined self-diffusion coefficients, is found to depend quantitatively on a limited set of material parameters: heat of adsorption, elastic modulus and percolation probability, all of which are experimentally accessible.

Diffusion of small molecules, e.g. water, in porous media is of fundamental importance for numerous applications including drug delivery, heterogeneous catalysis, adhesives, and many others. Diffusion is usually characterized by the diffusion coefficient. Supplementary Note S1 clarifies the many definitions of diffusion coefficient, including intrinsic, tracer, corrected, transport, mutual, self, chemical, and collective diffusion coefficients. Of note, this letter focuses on self-diffusion, or equivalently, tracer diffusion [1]. Understanding how diffusion coefficient is governed by the physical parameters of porous media has led to a plethora of mechanistic models ranging from activation [2,3], hopping [4], obstruction [5], free volume [6–8], to hydrodynamic/friction [9,10], etc.

For dilute polymer solutions, e.g. hydrogel (hydration typically higher than ~70%), diffusion theories are relatively well established as fluid-solid interactions can be reasonably neglected when pore size λ is much larger than the diffusant size σ, $\lambda >> \sigma$. For example, the obstruction theory successfully predicts diffusion coefficient in hydrogels by relating diffusion coefficient to the probability of finding a pore large enough to accommodate water molecules [5]. In contrast, for the case of highly concentrated polymer solutions, where $\lambda \sim \sigma$, the fluid-solid interaction force ζ becomes dominant as it roughly scales with the reciprocal of the pore length scale $\zeta \sim \lambda^{-1}$ (this is due to the fact that intermolecular solid/fluid forces are integrated over the entire specific surface area which scales as the pore surface to volume ratio). This strong fluid-solid interaction force leads to rich dynamics including molecular sieving, single-file diffusion, anomalous diffusion, etc [10]. Tortuous pore structure superimposes additional complexity on diffusion, whereas current diffusion theories have covered only simple pore geometries, such as cylindrical and planar pores [11]. In short, the strong fluid-solid interaction and complex pore structure form together a non-trivial energy landscape impeding the efforts of elucidating diffusion when the size of the pore, also referred to as mesh opening or free volume, approximates the water molecular size, $\lambda \sim \sigma$.

Besides the obstruction theory, researchers proposed free volume [6–8,12] and activation energy-based theories [8,13]. Molecular studies have proved that free volume scales linearly with adsorbed amount [12]. The experimental measurement of free volume remains sophisticated, involving positron annihilation lifetime spectroscopy [14], inverse gas chromatography [15], etc. [16], combined with semi-empirical interpretation. Though activation energy can be more easily measured through temperature-dependent Arrhenius processes [17,18], the connection between pore structure and activation energy, both relevant to diffusion, is not straightforward. Moreover, the above mentioned theories do not consider the intermittent dynamics of the diffusant. Previous works employed tortuosity, defined as the

ratio of self-diffusion coefficient of bulk water to water diffusion coefficient in pores $\xi = D_{s,w}/D_{\mu}$, to phenomenologically describe the intermittent dynamics (however, we note that this definition is not completely unambiguous as the in pore self-diffusivity can already differ from the bulk due to confinement effects – i.e. even in the absence of residence times at the pore surface). From a fundamental viewpoint, a microscopic explanation of tortuosity based on physical parameters is still lacking.

Continuum hypotheses break down at the subnanometer scale when $\lambda \sim \sigma$ [19]. In more detail, from a thermodynamical point of view, confined water displays a complex behavior as the interaction field generated by the host medium induces dynamical heterogeneities (e.g. [20]). From a dynamical point of view, rich dynamic boundaries and non-viscous effects lead to complex multiscale dynamics (e.g. [19,21]). To address water diffusion in a dense, sorptive and deformable polymer structure, this study resorts to molecular dynamics (MD). We first segregate microscopic diffusion coefficient from overall diffusion coefficient through the stop-and-go formalism – which is equivalent to the concept of intermittent Brownian motion – and then rationalize the concept of tortuosity using simple material parameters involving pore structure, sorption and deformation. Our approach provides a unifying picture of the intermittent motion of water molecules and of the quantification of complex diffusion landscape through physically well-defined material parameters. This model provides a way of predicting diffusion coefficients from adsorption heat, elastic modulus and percolation probability.

Six biopolymer systems are studied, i.e. two types of hemicelluloses, arabinoglucoronoxylan (AGX) and galactoglucomannan (GGM), two types of lignins, uncondensed lignin (uLGN) and condensed lignin (cLGN), and their mixtures, mixture 1 (M1, consisting of uLGN and AGX) and mixture 2 (M2, consisting of cLGN and GGM). These polymer structures present in wood are inspired and created following our previous work [22]. More details about the molecular models are included in Supplementary Note S2. These wood polymers are chosen as model systems because they cover a broad range of water-polymer interaction strengths, pore structures, chain connectivities, etc. Moreover, water diffusion in wooden materials is relevant to ubiquitous wooden building construction, furniture and artefacts, but also to more specialized issues including archeological wood preservation [23], advanced wood-based iontronics devices [24], etc. The moisture content, m, of the system is defined as the ratio of the mass of water to the mass of the dry polymer. This study focuses on a moisture content range m = 0-0.3, corresponding to the normal range of moisture load of wood exposed to humid environments [25]. Figure 1a shows a sample mixture system M2 consisting of GGM and cLGN at $m \sim 0.2$.

A typical simulation system has a lateral size of ~5 nm, containing ~10,000 atoms. The MD simulations are carried out using GROMACS 5.0 package [26] and GROMOS 53a6 united-atom force field [27] in isobaric-isothermal ensemble realized by velocity rescaling thermostat [28] and Berendsen barostat [29]. The simulation time of each system is 100-1000 ns depending on the time needed to reach the Fickian diffusion regime, i.e. where the mean square displacement (MSD) scales linearly with time. Sorption is mimicked by the random insertion method (Supplementary Note S2) [22].

Diffusion is usually described using Einstein's equation where particle diffusion is considered as random walk resulting from stochastic collisions. In sorptive systems, however, water molecules move via a series of waiting – sometimes referred to as residence/stop/immobile – and moving – relocation/go/mobile – events, alternatively identified as intermittent Brownian dynamics [2–4,10,30,31]. We also observe such behavior and include a sample MSD curve in Supplementary Note S3 (figure S1a) that displays alternating segments of plateaus and slopes, corresponding to waiting and moving status, respectively. Figure 1b is the schematic of the intermittent motion of a single water molecule.

Following our previous work [30], we define the time segment i, i.e. the time range $t_i < t < t_{i+1}$, as waiting if the deviation from the average displacement is less than 0.1 nm (OH bond length), $|\boldsymbol{r}(t) - \langle \boldsymbol{r} \rangle_t| < 0.1\ \text{nm}, t \in [t_i, t_{i+1}]$, and the rate of change of its squared displacement $\frac{\mathrm{d}\boldsymbol{r}^2(t)}{\mathrm{d}t} < 8 \times 10^{-8}\ \text{nm}^2\ \text{ns}^{-1}$, a value based on our visual observation of water trajectories. The waiting time $\tau_w = t_{i+1} - t_i$ is then averaged over all waiting segments and water molecules. The frequency of status switching, ν, is normalized by the total simulation time t_{tot}. Therefore, we have $t_{\text{tot}} = t_w + t_m = \tau_w \nu t_{\text{tot}} + \tau_m \nu t_{\text{tot}}$, where $\nu^{-1} = \tau_w + \tau_m$ [33] and τ_m is the moving time.

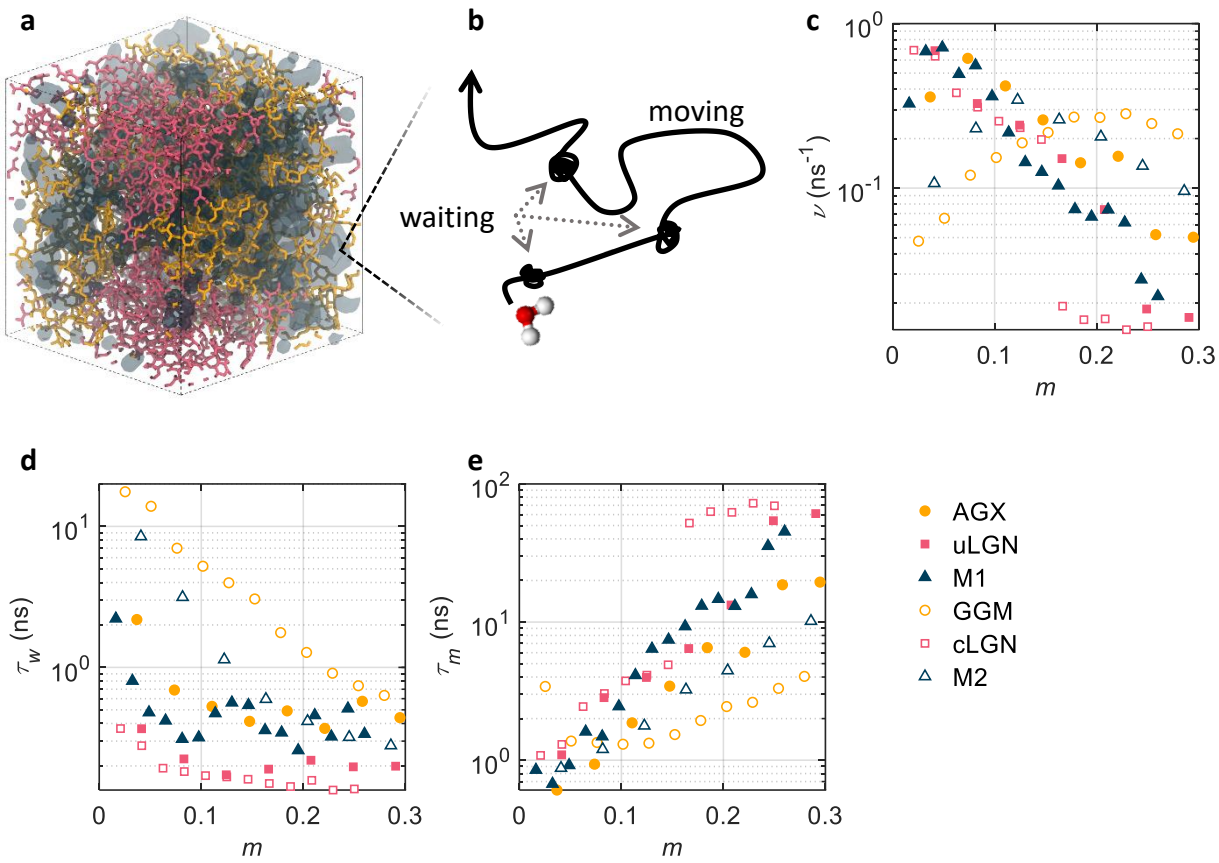

Figure 1 **a**) Sample system M2 at $m \sim 0.2$. The GGM, cLGN and water molecules are shown in yellow, pink and dark blue colors, respectively. **b**) Schematic of the intermittent motion of a single water molecule. **c**) Switching frequency ν. **d**) Waiting time τ_w. **e**) Moving time $\tau_m = \nu^{-1} - \tau_w$.

The switching frequency ν is shown as a function of moisture content in Figure 1c for all systems. For the lignins uLGN and cLGN, the switching frequency monotonically decreases with moisture content. With ongoing hydration process, adsorption sites at polymer surface are gradually occupied by water molecules and, therefore, the new water molecules in the system are gradually screened from adsorption at the occupied sites and consequently remain mostly more mobile. For the same reason, with increasing moisture content m, the waiting time τ_w decreases while moving time τ_m increases as shown in Figure 1d and e. The switching frequency of the hemicellulose-containing systems displays a peak at intermediate moisture contents. This peak implies a crossover from waiting dominated mode to moving dominated mode, meaning that water molecules mostly stay waiting at low moisture content due to sorption, and are mostly moving at high moisture content [32]. Here, ergodicity is implicitly invoked, meaning that the fractions of moving and waiting molecules equal to the fraction of moving and waiting phases, respectively.

In the waiting state, water molecules are trapped, thus displaying a nearly zero diffusion coefficient. The real displacement only occurs during the moving phases (while this behavior is observed here, we note that in general surface diffusion in the adsorbed state can also be found). The diffusion coefficient in the moving phase is referred to as microscopic diffusion coefficient $D_\mu = D/(\tau_m \nu)$ [30]. The factor $\tau_m \nu$ denotes the fraction of moving water or time with respect to the total number of water or total time. The microscopic diffusion coefficient D_μ and the fraction of moving water molecules $\tau_m \nu$ are shown in Figure 2a and b.

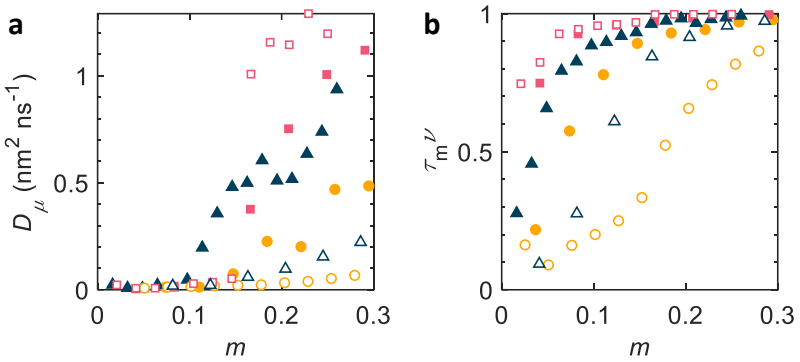

Figure 2 **a**) Microscopic diffusion coefficient. **b**) Fraction of moving water $\tau_m \nu$.

The diffusion coefficient D is calculated as the slope of the Fickian regime averaged over all water molecules and time origins (Supplementary Note S1). For all systems, the diffusion coefficients increase with increasing moisture content but remain lower than the bulk water self-diffusion coefficient $D_{s,w}$ = 3.5 nm^2 ns^{-1} (the bulk diffusion coefficient was measured in a separate simulation). The cLGN and uLGN show the highest diffusion coefficient while GGM the lowest. M1 shows a diffusion coefficient lower than uLGN but higher than AGX, i.e. a mixing of its two components, and so is M2. We note that the diffusion coefficient of cLGN surges at $m \sim 0.15$. This is attributed to a special type of water molecule structure, i.e. the formation of percolation, defined as the emergence of a water cluster that penetrates through the whole system creating a continued diffusion channel which greatly enhances diffusion coefficient.

According to Figure 2b, the more hydrophilic hemicelluloses, i.e. AGX and GGM, show a lower fraction of moving status. Nonetheless, at high moisture content, all systems approach nearly full moving status, i.e. $\tau_m \nu \sim 1$. This means that few water molecules remain waiting at higher moisture content. It further implies that the microscopic diffusion coefficient is actually close to the diffusion coefficient, i.e. $D_\mu \sim D$. The more diffusive systems not only have a larger

fraction of moving status, but also the water inside those systems moves faster as suggested by the higher D_μ.

The mobility status is found to correlate with the polymer-water distance d_{pw}, defined as the average distance between the oxygen atom of water and its nearest polymer atoms. The more mobile water molecules locate further away from polymer, $d_{pw,m} > d_{pw,w}$, shown in figure S4. Furthermore, d_{pw} can characterize the dispersity of water because it is related to the ratio of the number of water at the surface of the cluster to the total number of water of the cluster, a common measure of dispersity. Based on our results, water in hemicelluloses disperses better than in lignins, a behavior which agrees with previous reports [22].

In the following, we analyse the behavior of the ratio $D_\mu/D_{s,w}$, which is the microscopic diffusion coefficient D_μ normalized by the bulk self-diffusion coefficient, referred to as the normalized diffusion coefficient. We note that the reciprocal of $D_\mu/D_{s,w}$ is often referred to as tortuosity, $\xi = D_{s,w}/D_\mu$, interpreted as the degree of "detour" of the path taken by a diffusing water molecule caused by the tortuous pore space. The normalized diffusion coefficient is usually less than 1, $\xi^{-1} < 1$, because the diffusion coefficient in porous media is generally less than the bulk self-diffusion coefficient of liquid water under the same thermodynamic conditions.

Nanoporous biopolymer systems could represent sorptive, deformable and nanoporous structures. This letter attempts to offer an alternative view of diffusion utilizing sorption and deformability, which are quantitatively represented by adsorption heat Q_{ad} and elastic moduli E, respectively. Measurement methods and results of these properties are described in Supplementary Note S4 (figure S2). The normalized diffusion coefficient or tortuosity are exponential functions of adsorption heat and elastic moduli, the justification of which is discussed as follows.

In the activation theory, diffusion coefficient scales with the activation energy E_a, $D \sim \exp(-E_a/k_B T)$. One can invoke a linear relationship between activation energy E_a of diffusion and heat of adsorption, $E_a \sim \alpha Q_{ad}$ [33] (with α of the order but larger than 1 – in other words, the energy barrier is larger than the energy differnce between two states). Therefore, taking the limit $\alpha = 1$, an exponential relation between normalized diffusion coefficient can be employed, $\xi^{-1} \sim \exp(-Q_{ad}/k_B T)$, where k_B and T denote Boltzmann constant and temperature, respectively. This relation is shown to be valid, as seen in Figure 3b. It should be noted that in this study we take liquid water as the reference state.

Yang and Chun derived the relation between diffusion coefficient and polymer persistence length ln $D \sim l_p^{1/2}$ [34]. The persistence length of a worm-like chain is related to Young's modulus E, cross-section area, and moment of inertia M, following the relation $l_p = EM/k_BT$ [35]. Therefore the normalized diffusion coefficient is also assumed to scale exponentially with Young's modulus, $\xi^{-1} \sim \exp[(E/E_0)^{1/2}]$, where E_0 is for simplicity equal to 1 GPa only for making the term between brackets dimensionless. Figure 3c shows the validity of the proposed exponential scaling.

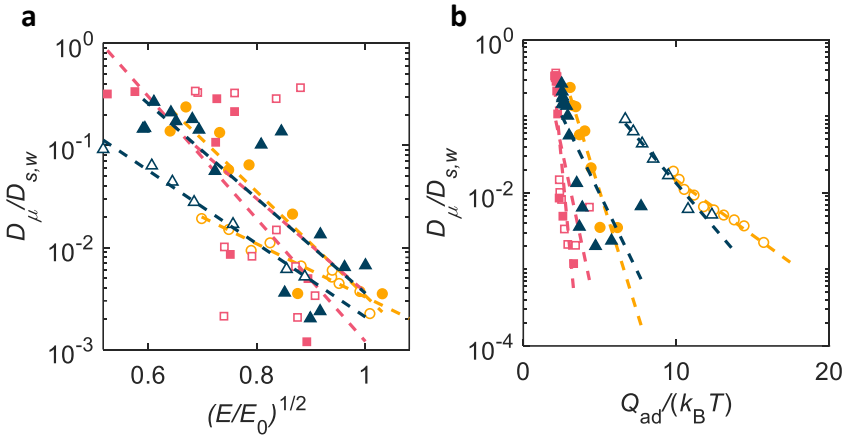

Figure 3 Normalized diffusion coefficient in relation to **a**) heat of adsorption Q_{ad}/k_BT and **b**) Young's modulus $(E/E_0)^{1/2}$ in a semi-log plot.

The prediction of diffusion coefficient based on heat of adsorption and elastic moduli works relatively well, as shown in Supplementary Note S5. However, for some systems, e.g. cLGN, there exists a surge of diffusion coefficient around $m \sim 0.15$, which is related to the occurrence of percolation. The prediction above, which relies on two terms (heat of adsorption and persistence length), fails to include such feature. It is thus necessary to introduce percolation into the model.

In this study, percolation is quantified by the percolation probability p_p defined as the time interval during which percolation is occurring divided by the total simulation time, i.e. $p_p = \int \delta_p(t)dt \,/\, \int dt$, where $\delta_p(t_i)$ equals 1 or 0 whether or not the system percolates at time t_i, correspondingly (details in Supplementary Note S4). The scaling between normalized diffusion coefficient and percolation probability p_p is not a simple function. In analogy with heat of adsorption and modulus, we propose an exponential scaling, $\xi^{-1} \sim \exp(p_p)$ (it will be shown afterwards that this mathematical form provides a reasonable description of the obtained results). In essence, percolation is a special type of structural feature that is not represented by heat of adsorption heat and elastic modulus, which support the inclusion of percolation as a separate

factor. The percolation probability is system size dependent. This study focuses on dense polymer networks with nanoscale pores which minimizes the impact of the size effect.

In spirit of tortuosity factorization [36], the abovementioned factors are multiplied in the sorption-deformation-percolation (SDP) model:

$$\frac{1}{\exp(a_0)}\cdot\frac{D_\mu}{D_{s,w}} = \exp\left(a_Q\frac{Q_{\mathrm{ad}}}{k_{\mathrm{B}}T}\right)\cdot\exp\left(a_E\left(\frac{E}{E_0}\right)^{1/2}\right)\cdot\exp\left(a_{\mathrm{p}}p_{\mathrm{p}}\right) \tag{221}$$

where a_{i} (i = 0, Q, E or p) is weight. We can also write

$$\ln\frac{D_\mu}{D_{s,w}} = a_0 + a_Q\frac{Q_{\mathrm{ad}}}{k_{\mathrm{B}}T} + a_E\left(\frac{E}{E_0}\right)^{1/2} + a_{\mathrm{p}}p_{\mathrm{p}}$$

The SDP model well describes the measurements as shown in Figure 4. A sensitivity analysis is carried out by omitting an arbitrary number of factors. The prediction power is poor for any model with fewer factors.

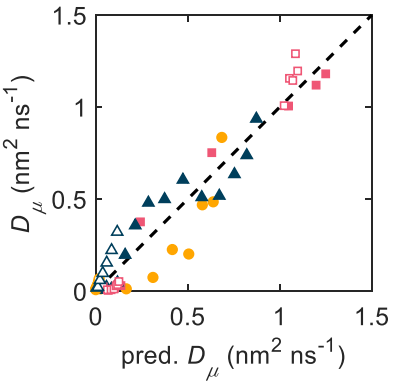

Figure 4 Measured and predicted diffusion coefficient D_μ.

The weights are a_0 = -0.572, a_Q = -3.051, a_E = -1.243 and a_{p} = 0.466. The weights a_{i} in the SDP model are dimensionless numbers, which are the first derivative of $\ln\xi^{-1}$ with respect to the corresponding property x_{i}, $a_{\mathrm{i}}=\partial\ln\xi^{-1}/\partial x_{\mathrm{i}}$. The a_0 is introduced to manifest all the influencing factors other than sorption, deformation and percolation. Especially, when a_Q is zero, the SDP model reduces to the description of non-sorptive material. Previous diffusion models generally focus on systems where host-guest interaction is negligible and the pore length scale is much larger than the diffusant size. Here we show that the SDP model well describes dense, sorptive and deformable polymer materials, e.g. nanoporous biopolymers.

The model can potentially be verified by experiments. Diffusion coefficient D can be measured via nuclear magnetic resonance (NMR). The waiting and moving statistics are accessible via experimental methods such as differential scanning calorimetry (DSC) and NMR [37]. In fact,

our simulation shows that water in most systems is mainly in the moving state, except for the strongly adsorbing material, GGM, whose heat of adsorption reaches ~43 kJ mol^{-1}. It is noted that the latent heat of water is not included as we use liquid water as the reference state (details in Supplementary Note S4). The proposed material parameters of tortuosity are also experimentally accessible: heat of adsorption Q_{ad} and Young's modulus E can be measured via calorimetry and mechanical tests, respectively; the probability of percolation can be estimated by e.g. conductivity or capacitance. Preliminary validation of the SDP model based on literature data is included in Supplementary Note S7 where acceptable agreement between the predicted and measured diffusion coefficient is shown.

While this study focuses on water diffusion, we believe that our framework can be extended to other diffusants, such as hydrated ions, methane, etc., as long as the molecular size approximates the size of the free volume or pore length scale. For instance, most drugs have molecular sizes around 0.5-5 nm which are comparable to the pore length scale of the drug delivery systems. Better control of drug release can be achieved by the rational design of the structure of the host porous media under the guidance of our model.

The polymer-water distance d_{pw} is found to be strongly correlated with heat of adsorptionQ_{ad}, as shown in figure S4. This offers an alternative way of characterizing sorption. Replacing Q_{ad} with d_{pw} in SDP model give equivalently good results, which further demonstrates that they carry the same information and can thus be used interchangeably.

To sum up, this study offers a unifying picture of water diffusion within dense disordered porous media, and moreover describes diffusion coefficient via a complete set of physically well-defined material properties. We resort to MD simulations where the trajectories of individual water molecules manifest the intermittent dynamics which is caused by strong sorption interactions and highly tortuous pore space. The microscopic diffusion coefficient D_μ should be extracted from the measured diffusion coefficient D by disregarding the waiting phases using factor $\tau_m v$, the fraction of moving water derived from single water molecule statistics. The microscopic diffusion coefficient, equivalently tortuosity ξ, is then predicted via three characteristic parameters of the porous media, i.e. heat of adsorption Q_{ad}, Young's modulus E and probability of percolation p_p, each representing a fundamental physical aspect of the porous system, i.e. sorption, deformation and percolating structure. The SDP model, therefore, provides guidelines for the comparison of diffusion in different polymers. The model may guide the design of materials to achieve desired diffusion property.

Supplementary material:

Funding: The authors acknowledge the support of the Swiss National Science Foundation (SNSF) [grant No. 162957].

References

[1] J. Kärger and D. M. Ruthven, *Diffusion in Nanoporous Materials: Fundamental Principles, Insights and Challenges*, New J. Chem. **40**, 4027 (2016).

[2] A. T. DiBenedetto and D. R. Paul, *An Interpretation of Gaseous Diffusion through Polymers Using Fluctuation Theory*, J. Polym. Sci. Part A Gen. Pap. **2**, 1001 (1964).

[3] P. Meares, *The Diffusion of Gases Through Polyvinyl Acetate 1*, J. Am. Chem. Soc. **76**, 3415 (1954).

[4] F. M. Preda, A. Alegría, A. Bocahut, L. A. Fillot, D. R. Long, and P. Sotta, *Investigation of Water Diffusion Mechanisms in Relation to Polymer Relaxations in Polyamides*, Macromolecules **48**, 5730 (2015).

[5] N. A. Hadjiev and B. G. Amsden, *An Assessment of the Ability of the Obstruction-Scaling Model to Estimate Solute Diffusion Coefficients in Hydrogels*, J. Control. Release **199**, 10 (2015).

[6] J. S. Vrentas and J. L. Duda, *Diffusion in Polymer—Solvent Systems. I. Reexamination of the Free-Volume Theory*, J. Polym. Sci. Polym. Phys. Ed. **15**, 403 (1977).

[7] H. Fujita, *Diffusion in Polymer-Diluent Systems*, in *Fortschritte Der Hochpolymeren-Forschung* (Springer-Verlag, Berlin/Heidelberg, 1961), pp. 1–47.

[8] K. Falk, B. Coasne, R. Pellenq, F. J. Ulm, and L. Bocquet, *Subcontinuum Mass Transport of Condensed Hydrocarbons in Nanoporous Media*, Nat. Commun. **6**, 6949 (2015).

[9] R. I. Cukier, *Diffusion of Brownian Spheres in Semidilute Polymer Solutions*, Macromolecules **17**, 252 (1984).

[10] C. Bousige, P. Levitz, and B. Coasne, *Bridging Scales in Disordered Porous Media by Mapping Molecular Dynamics onto Intermittent Brownian Motion*, Nat. Commun. **12**, 1 (2021).

[11] B. Coasne, *Multiscale Adsorption and Transport in Hierarchical Porous Materials*, New J. Chem. **40**, 4078 (2016).

[12] A. Obliger, R. Pellenq, F.-J. Ulm, and B. Coasne, *Free Volume Theory of Hydrocarbon Mixture Transport in Nanoporous Materials*, J. Phys. Chem. Lett. **7**, 3712 (2016).

[13] R. M. Barrer, *The Zone of Activation in Rate Processes*, Trans. Faraday Soc. **39**, 237 (1943).

[14] G. Dlubek, A. P. Clarke, H. M. Fretwell, S. B. Dugdale, and M. A. Alam, *Positron Lifetime Studies of Free Volume Hole Size Distribution in Glassy Polycarbonate and Polystyrene*, Phys. Status Solidi Appl. Res. **157**, 351 (1996).

[15] Y. P. Yampolskii, N. E. Kaliuzhnyi, and S. G. Durgarjan, *Thermodynamics of Sorption in Glassy Poly(Vinyltrimethylsilane)*, Macromolecules **19**, 846 (1986).

[16] J. C. Jansen, M. MacChione, E. Tocci, L. De Lorenzo, Y. P. Yampolskii, O. Sanfirova, V. P. Shantarovich, D. Hofmann, and E. Drioli, *Comparative Study of Different Probing Techniques for the Analysis of the Free Volume Distribution in Amorphous Glassy Perfluoropolymers*, Macromolecules **42**, 7589 (2009).

[17] W. W. Brandt, *Model Calculation of the Temperature Dependence of Small Molecule Diffusion in High Polymers*, J. Phys. Chem. **63**, 1080 (1959).

[18] A. T. DiBenedetto, *Molecular Properties of Amorphous High Polymers. II. An Interpretation of Gaseous Diffusion through Polymers*, J. Polym. Sci. Part A Gen. Pap. **1**, 3477 (1963).

[19] L. Bocquet and E. Charlaix, *Nanofluidics, from Bulk to Interfaces*, Chem. Soc. Rev. **39**, 1073 (2010).

[20] B. Coasne, A. Galarneau, F. Di Renzo, and R. J. M. Pellenq, *Molecular Simulation of Adsorption and Intrusion in Nanopores*, Adsorption **14**, 215 (2008).

[21] C. Cottin-Bizonne, J. L. Barrat, L. Bocquet, and E. Charlaix, *Low-Friction Flows of Liquid at Nanopatterned Interfaces*, Nat. Mater. **2**, 237 (2003).

[22] C. Zhang, M. Chen, S. Keten, B. Coasne, D. Derome, and J. Carmeliet, *Hygromechanical Mechanisms of Wood Cell Wall Revealed by Molecular Modeling and Mixture Rule Analysis*, Sci. Adv. **7**, (2021).

[23] E. Hocker, G. Almkvist, and M. Sahlstedt, *The Vasa Experience with Polyethylene Glycol: A Conservator's Perspective*, J. Cult. Herit. **13**, S175 (2012).

[24] T. Li et al., *A Nanofluidic Ion Regulation Membrane with Aligned Cellulose Nanofibers*, Sci. Adv. **5**, eaau4238 (2019).

[25] A. J. Stamm, *Wood and Cellulose Science* (Ronald, 1964).

[26] M. J. Abraham, T. Murtola, R. Schulz, S. Páll, J. C. Smith, B. Hess, and E. Lindah, *Gromacs: High Performance Molecular Simulations through Multi-Level Parallelism from Laptops to Supercomputers*, SoftwareX **1**–**2**, 19 (2015).

[27] C. Oostenbrink, A. Villa, A. E. Mark, and W. F. Van Gunsteren, *A Biomolecular Force Field Based on the Free Enthalpy of Hydration and Solvation: The GROMOS Force-Field Parameter Sets 53A5 and 53A6*, J. Comput. Chem. **25**, 1656 (2004).

[28] G. Bussi, D. Donadio, and M. Parrinello, *Canonical Sampling through Velocity Rescaling*, J. Chem. Phys. **126**, 014101 (2007).

[29] H. J. C. Berendsen, J. P. M. Postma, W. F. van Gunsteren, A. DiNola, J. R. Haak, J. P. M. van Postma, W. F. van Gunsteren, A. DiNola, and J. R. Haak, *Molecular Dynamics with Coupling to an External Bath*, J. Chem. Phys. **81**, 3684 (1984).

[30] K. Kulasinski, R. Guyer, D. Derome, and J. Carmeliet, *Water Diffusion in Amorphous Hydrophilic Systems: A Stop and Go Process*, Langmuir **31**, 10843 (2015).

[31] A. Malani and K. G. Ayappa, *Relaxation and Jump Dynamics of Water at the Mica Interface*, J. Chem. Phys. **136**, 194701 (2012).

[32] C. Zhang, B. Coasne, R. Guyer, D. Derome, and J. Carmeliet, *Moisture-Induced Crossover in the Thermodynamic and Mechanical Response of Hydrophilic Biopolymer*, Cellulose **27**, 89 (2020).

[33] V. J. Inglezakis and A. A. Zorpas, *Heat of Adsorption, Adsorption Energy and Activation Energy in Adsorption and Ion Exchange Systems*, Desalin. Water Treat. **39**, 149 (2012).

[34] Y. Yang and M.-S. Chun, *The Effect of Chain Stiffness on Moisture Diffusion in Polymer Hydrogel by Applying Obstruction-Scaling Model*, Korea-Australia Rheol. J. **25**, 267 (2013).

[35] C. G. Baumann, S. B. Smith, V. A. Bloomfield, and C. Bustamante, *Ionic Effects on the Elasticity of Single DNA Molecules*, Proc. Natl. Acad. Sci. **94**, 6185 (1997).

[36] A. Boţan, F.-J. Ulm, R. J.-M. Pellenq, and B. Coasne, *Bottom-up Model of Adsorption and Transport in Multiscale Porous Media*, Phys. Rev. E **91**, 032133 (2015).

[37] T. Hatakeyama, M. Tanaka, A. Kishi, and H. Hatakeyama, *Comparison of Measurement Techniques for the Identification of Bound Water Restrained by Polymers*, Thermochim. Acta **532**, 159 (2012).